Water Oxidation Hot Paper

Deutsche Ausgabe: DOI: 10.1002/ange.201602764
Internationale Ausgabe: DOI: 10.1002/anie.201602764

Modification of Wide-Band-Gap Oxide Semiconductors with Cobalt Hydroxide Nanoclusters for Visible-Light Water Oxidation

Kazuhiko Maeda, Koki Ishimaki, Yuki Tokunaga, Daling Lu, and Miharu Eguchi*

Abstract: *Cobalt-based compounds, such as cobalt(II) hydroxide, are known to be good catalysts for water oxidation. Herein, we report that such cobalt species can also activate wide-band-gap semiconductors towards visible-light water oxidation. Rutile TiO_2 powder, a well-known wide-band-gap semiconductor, was capable of harvesting visible light with wavelengths of up to 850 nm, and thus catalyzed water oxidation to produce molecular oxygen, when decorated with cobalt(II) hydroxide nanoclusters. To the best of our knowledge, this system constitutes the first example that a particulate photocatalytic material that is capable of water oxidation upon excitation by visible light can also operate at such long wavelengths, even when it is based on earth-abundant elements only.*

Artificial photosynthesis has long attracted significant attention in diverse fields of science as a potential means of producing fuel from renewable resources.[1–5] In artificial photosynthetic schemes for fuel generation (such as water splitting and CO_2 fixation), the formation of O_2 by water oxidation is recognized as the most difficult step as it involves a four-electron process that is kinetically slow.[6–9]

Photocatalytic reactions using powder-based semiconductor materials are attractive from the viewpoint of large-scale applications because of their simplicity and scalability.[10] Certain metal oxides containing d^0 or d^{10} transition-metal cations are stable semiconductor photocatalysts for water oxidation, allowing for overall water splitting under band-gap irradiation.[11] However, because most of the reported metal oxide photocatalysts have a large band gap, which originates from the deep valence-band potential, with respect to the water oxidation potential, these systems are largely insensitive to visible light.[12] For example, rutile TiO_2 exhibits high water oxidation activity upon band-gap excitation by UV light ($\lambda < 400$ nm), yet it is almost inactive under visible-light irradiation.[13]

To expand the utility of these photocatalysts, several groups have developed systems that have greater efficiency in the visible region. Maeda and Domen developed several non-oxide photocatalysts, including oxynitrides, nitrides, and oxysulfides, that are designed to split water upon excitation by visible light.[14] Zhang, Li et al. reported that $LaTiO_2N$ and Ta_3N_5 coupled with CoO_x nanoparticle cocatalysts showed very high apparent quantum efficiencies (AQEs) for water oxidation under visible excitation at wavelengths as long as 600 nm.[15] Recent progress has seen the spectral ranges of both oxynitride[16–18] and oxide[4] systems being further extended into the visible region. Thus far, the spectral range of a perovskite oxynitride of $BaNbO_2N$ modified with a CoO_x cocatalyst has extended furthest into the visible region, utilizing wavelengths of up to 740 nm to facilitate catalysis.[18] However, no powder photocatalyst has been reported to utilize light of $\lambda > 800$ nm for water oxidation. The development of such catalysts undoubtedly constitutes a major challenge, particularly when using earth-abundant elements only.

Aside from increasing the efficacy of these photocatalysts by expanding their spectral absorption range, other groups have made further advances in developing more effective oxidation catalysts.[8] A report by Kanan and Nocera in 2008[19] made cobalt-based compounds popular candidates for efficient, earth-abundant water oxidation by photocatalysis[15,18,20–22] and (photo)electrolysis.[6,23–25] A number of papers describe an increase in catalytic activity and performance as a result of the presence of cobalt-based cocatalyst nanoparticles on a semiconducting material. These nanoparticles act as catalytic sites for water oxidation by accepting holes that were photogenerated in the valence band of the semiconductor.[15,25]

In the present study, our aim was to develop an effective photocatalyst based on earth-abundant cobalt and titanium. Specifically, we explored the dual functionality of a cobalt compound as both a water oxidation cocatalyst and a photoabsorber that excites a wide-band-gap metal oxide powder such as TiO_2. Utilizing ubiquitous elements to create a new material that exhibits outstanding functionality is one of the most important missions in chemistry. Herein, we show that rutile TiO_2 nanorods decorated with approximately 2 nm large $Co(OH)_2$ nanoclusters are capable of oxidizing water into O_2 under visible-light irradiation at wavelengths of up to 850 nm, which is the longest wavelength ever reported for water oxidation with a heterogeneous photocatalyst. Furthermore, this strategy of using $Co(OH)_2$ for visible-light water

[*] Prof. Dr. K. Maeda, K. Ishimaki, Y. Tokunaga
Department of Chemistry, School of Science
Tokyo Institute of Technology
2–12-1-NE-2 Ookayama, Meguro-ku, Tokyo 152-8550 (Japan)
E-mail: maedak@chem.titech.ac.jp
Dr. D. Lu
Center for Advanced Materials Analysis
Tokyo Institute of Technology
4259 Nagatsuta-cho, Midori-ku, Yokohama 226-8503 (Japan)
Dr. M. Eguchi
Electronic Functional Materials Group
Polymer Materials Unit
National Institute for Materials Science
1-1 Namiki, Tsukuba, Ibaraki 305-0044 (Japan)

Supporting information for this article can be found under: http://dx.doi.org/10.1002/anie.201602764.

 © 2016 Wiley-VCH Verlag GmbH & Co. KGaA, Weinheim

oxidation could be applicable to some other wide-band-gap semiconductors such as anatase TiO_2 and $KTiNbO_5$.

$Co(OH)_2/TiO_2$ inorganic hybrids were prepared by an impregnation/precipitation method (see the Supporting Information for details). Briefly, rutile TiO_2 powder was sonicated in an aqueous solution containing $Co(NO_3)_2$ at room temperature for 10 min. An aqueous NH_3 solution (28 vol%) was then added dropwise to the suspension, and the resulting reaction mixture was evaporated and dried in an oven at 343 K overnight to yield a brown solid. Note that $Co(OH)_2$ is thermally stable at temperatures below 343 K, and not transformed into other phases with higher oxidation states, such as Co_3O_4.[26]

X-ray diffraction (XRD) patterns for the as-prepared materials with different $Co(OH)_2$ contents are shown in the Supporting Information, Figure S1. From now on, the composition of the materials will be referred to in terms of the weight percentage of the cobalt species. For example, a 3.0 wt% $Co(OH)_2/TiO_2$ sample contains 3.0 wt% of $Co(OH)_2$. All of the synthesized materials exhibited a single-phase diffraction pattern, which was assigned to rutile TiO_2. No peaks that are due to Co species were observed even for the 10.0 wt% $Co(OH)_2/TiO_2$ samples. However, X-ray photoelectron spectroscopy (XPS) analysis of the catalyst (Figure S2) revealed a Co $2p_{3/2}$ binding energy of 781.4 eV, which agrees with that expected for Co^{II} in $Co(OH)_2$.[21,27,28] The satellite peak at 787.2 eV is another indication of the inclusion of Co^{II} species.[15a]

The rutile TiO_2 nanorods developed in this study had an average diameter of approximately 10 nm and an average length of about 50 nm (Figure 1). The specific surface area was calculated to be 85 m^2g^{-1} by a nitrogen adsorption measurement conducted at liquid nitrogen temperature. Analysis by high-resolution transmission electron microscopy (HR-TEM) showed that in the 3.0 wt% $Co(OH)_2/TiO_2$ sample, the $Co(OH)_2$ particles had been deposited on the TiO_2 surface as highly dispersed, approximately 2 nm nanoclusters. The presence of cobalt was confirmed by energy-dispersive X-ray spectroscopy (Figure S3). At a $Co(OH)_2/TiO_2$ loading of 10.0 wt%, however, the surface coverage by approximately 2 nm large nanoclusters was more pronounced, causing some aggregation of $Co(OH)_2$ to yield larger secondary particles. Some of the deposited $Co(OH)_2$ nanoclusters show lattice fringes separated by about 0.23 nm, which is consistent with the *d* spacing of the (001) planes in $Co(OH)_2$ (Figure S4).

We also prepared $Co(OH)_2/SiO_2$ as a reference compound in a similar manner. The UV/Vis diffuse reflectance spectrum and the color (pale pink) of $Co(OH)_2/SiO_2$ resemble those of a bulk β-$Co(OH)_2$ reference (Figure S5) although the spectral shape is not very sharp compared to that of the reference compound, which is primarily due to the low $Co(OH)_2$ concentration. These results indicate that the Co species thus prepared were $Co(OH)_2$.

On the basis of these results, it is reasonable to conclude that the valence state of the Co species on TiO_2 generally is Co^{II}. However, we could not completely rule out the presence of Co^{III} species in the products, as the surface of $Co(OH)_2$ may undergo oxidation in air.

The optical absorption properties of the material were assessed by UV/Vis diffuse reflectance spectroscopy (DRS). As shown in Figure 2, pristine rutile TiO_2 hardly absorbs visible light. However, the $Co(OH)_2/TiO_2$ system had an absorption band extending to 850 nm, accounting for the brown color of the material. The intensity of the absorption band increased as the concentration of cobalt was increased. The absorption feature that corresponds to d–d transitions in the Co^{II} species at around 550 nm for $Co(OH)_2$ (Figure S5) almost disappeared after immobilization on the TiO_2 surface. Furthermore, the absorption features of $Co(OH)_2/TiO_2$ were not observed when $Co(OH)_2$ and TiO_2 were physically mixed (Figure 2). These results suggest that there is a relatively strong electronic interaction between $Co(OH)_2$ and TiO_2, which contributes to the visible-light absorption of the $Co(OH)_2/TiO_2$ material. The energy gap of $Co(OH)_2/TiO_2$ was estimated to be approximately 1.5 eV from the onset wavelength (800–850 nm) of the absorption.

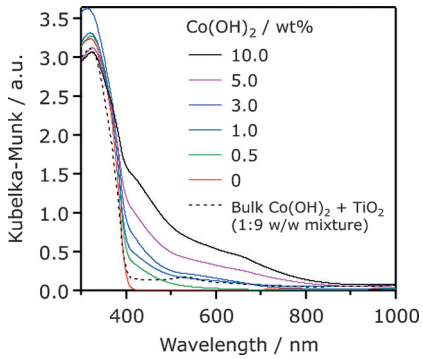

Figure 2. UV/Vis diffuse reflectance spectra of $Co(OH)_2/TiO_2$ with different amounts of $Co(OH)_2$. Data for a mixture of bulk $Co(OH)_2$ and TiO_2 (1:9, w/w) are shown for comparison.

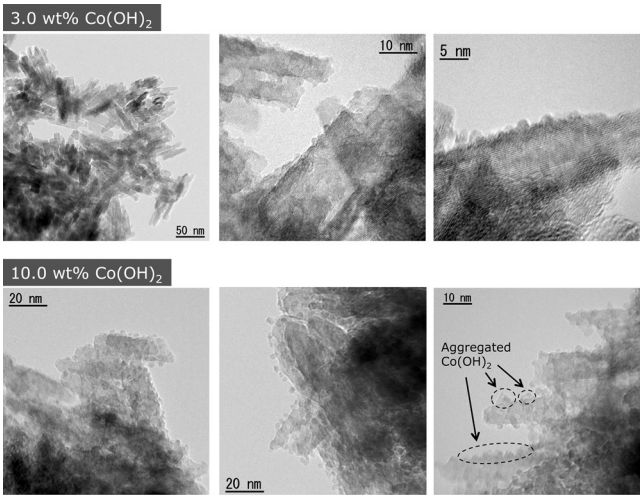

Figure 1. TEM images of 3.0 wt% and 10.0 wt% $Co(OH)_2/TiO_2$.

The $Co(OH)_2/TiO_2$ nanohybrids were used to photocatalytically oxidize water in an aqueous solution containing Ag^+ and La_2O_3 under visible-light irradiation ($\lambda > 500$ nm). Ag^+

© 2016 Wiley-VCH Verlag GmbH & Co. KGaA, Weinheim

and La_2O_3 act as electron acceptor and pH buffer, respectively.[15–18] Reactions in the presence of Ag^+ as an electron acceptor are an established means of evaluating the photocatalytic water oxidation activity of a semiconductor.[15–18,29–32] As shown in Table 1, rutile TiO_2 exhibited little photocatalytic

Table 1: O_2 evolution rates over $Co(OH)_2/TiO_2$ under visible-light irradiation ($\lambda > 500$ nm).[a]

Entry	Sample	$Co(OH)_2$ loading [wt%]	O_2 evolution rate [$\mu mol\,h^{-1}$]
1	TiO_2	–	N.D.
2	$Co(OH)_2/SiO_2$	3.0	N.D.
3	$Co(OH)_2/TiO_2$	0.5	1
4	$Co(OH)_2/TiO_2$	1.0	3
5	$Co(OH)_2/TiO_2$	3.0	11
6	$Co(OH)_2/TiO_2$	5.0	5
7	$Co(OH)_2/TiO_2$	10.0	3
8[b]	$Co(OH)_2/TiO_2$	3.0	N.D.
9	bulk $Co(OH)_2$	–	0.2
10[c]	bulk $Co(OH)_2$ and TiO_2	–	2
11[d]	reduced TiO_2	–	N.D.

[a] Reaction conditions: Catalyst (100 mg), reactant solution, aqueous silver nitrate solution (10 mM, 140 mL) containing 200 mg of La_2O_3, 300 W xenon lamp with a cut off filter (Y-50). [b] In the dark. [c] A physical mixture of 50 mg bulk $Co(OH)_2$ and 50 mg TiO_2. [d] Prepared by heating TiO_2 at 973 K for 1 h under a flow of H_2 (20 $mL\,min^{-1}$). See the XRD and DRS data in Figure S6.

activity under these conditions, primarily owing to its large band gap. $Co(OH)_2/SiO_2$ also showed no activity. However, when $Co(OH)_2$ and TiO_2 were combined, O_2 evolution was observed. Furthermore, the water oxidation activity depended on the amount of $Co(OH)_2$. The O_2 evolution from $Co(OH)_2/TiO_2$ increased with an increase in Co loading up to 3.0 wt% $Co(OH)_2/TiO_2$. Above this loading, the catalytic activity decreased, possibly because of the excess coverage of the rutile nanorod surfaces and/or aggregation of the $Co(OH)_2$ nanoclusters (Figure 1). The system did not evolve O_2 when not exposed to light. Note that bulk $Co(OH)_2$ showed little, but observable O_2 evolution under the present conditions (entry 9), indicating that $Co(OH)_2$ itself had a low level of photocatalytic water oxidation activity. Interestingly, a physical mixture of bulk $Co(OH)_2$ and TiO_2 (entry 10) gave a higher rate of O_2 evolution than bulk $Co(OH)_2$, although the activity was generally lower than those recorded for $Co(OH)_2/TiO_2$ composites (entries 4–7). These results indicate that the interaction between $Co(OH)_2$ and TiO_2 is essential for the visible-light water oxidation activity. Importantly, a reduced TiO_2 sample with mid-gap state(s) in its band-gap structure did not show activity under the same reaction conditions (Figure S6). This result strongly suggests that light absorption from mid-gap states does not contribute to the visible-light water oxidation activity.

The role of rutile TiO_2 in the visible-light water oxidation reaction was also investigated. We prepared rutile samples with smaller specific surface areas by simply heating the original rutile nanorods in air at elevated temperatures. The heat treatment resulted in the generation of aggregated rutile particles (Figure S7).

The heated samples were then tested for O_2 evolution in combination with different amounts of $Co(OH)_2$. The O_2 evolution rate tended to decrease with a decrease in the specific surface area of TiO_2 (Table S1). The activity of the 973 K sample with a $Co(OH)_2$ loading of 3.0 wt% was lower than that of the 1.0 wt% sample. With the 1273 K sample, O_2 evolution was not detected, regardless of the loading amount. It becomes difficult to achieve highly dispersed catalytic nanoparticles when the specific surface of a support is low.[11a] In the present reaction scheme, more $Co(OH)_2$ is required for visible-light harvesting. However, when too much $Co(OH)_2$ is introduced and/or the TiO_2 surface area is small, the $Co(OH)_2$ particles will aggregate, which reduces the catalytic activity.

Thus, TiO_2 was concluded to serve as a support to disperse $Co(OH)_2$ on the surface and accept electrons from the $Co(OH)_2$ light-harvesting antenna. To achieve this, nanosized TiO_2 with a high surface area would be ideal to accommodate more $Co(OH)_2$ with an optimal distribution. It is likely that an increase in the contact area between $Co(OH)_2$ and TiO_2 will enhance the overall activity, although we could not evaluate this effect quantitatively because of the aggregated nature of the TiO_2 samples (Figures 1 and S7). Charge transfer from $Co(OH)_2$ to TiO_2 was also confirmed by means of a photoelectrochemical technique. As shown in Figure 3, the

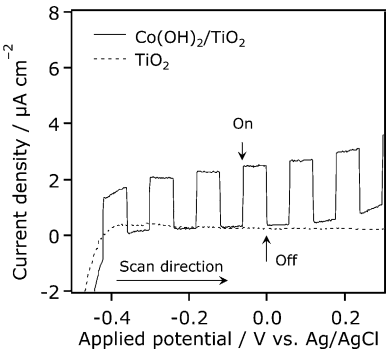

Figure 3. Current–voltage curves in aqueous 0.1 M Na_2SO_4 solution (pH 8–9) under intermittent visible-light irradiation ($\lambda > 500$ nm) for $Co(OH)_2/TiO_2$ and TiO_2 electrodes (5.25 cm^2). Scan rate: 20 $mV\,s^{-1}$.

$Co(OH)_2/TiO_2$ electrode exhibited an anodic photoresponse under visible-light irradiation ($\lambda > 500$ nm). On the other hand, no photoresponse was observed for an unmodified TiO_2 electrode under the present conditions whereas it gave an appreciable photocurrent under band-gap irradiation.[33] The visible-light-induced anodic photocurrent is a clear indication of electron transfer from $Co(OH)_2$ to the conduction band of TiO_2 because of the upward band bending of TiO_2 that originates from its n-type semiconductor properties.

On the basis of the diffuse reflectance spectroscopy results and the photoelectrochemical measurements, an energy diagram for $Co(OH)_2/TiO_2$ was constructed (Figure 4). As the conduction band minimum of rutile TiO_2 is located at a potential very close to the water reduction potential (ca. 0 V vs. NHE at pH 0),[34] the tops of the occupied levels formed by $Co(OH)_2$ are approximately 1.5 V more positive than the conduction band minimum of TiO_2. The energy diagram

 © 2016 Wiley-VCH Verlag GmbH & Co. KGaA, Weinheim

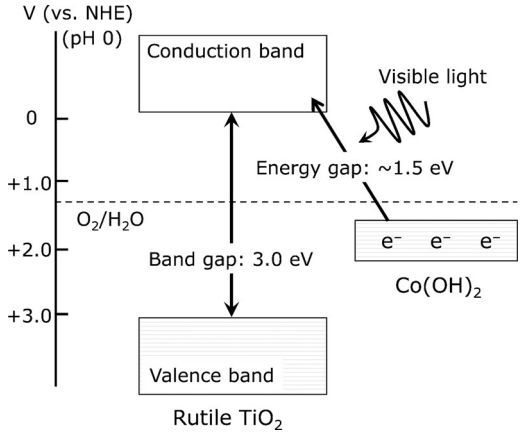

Figure 4. Proposed energy diagram for $Co(OH)_2/TiO_2$.

indicates that $Co(OH)_2/TiO_2$ satisfies the thermodynamic requirements for oxidizing water and reducing Ag^+, which is in good agreement with the results of the photocatalytic reactions (Table 1).

Figure 5 shows the time dependence of the O_2 evolution over 3.0 wt% $Co(OH)_2/TiO_2$ under visible-light irradiation ($\lambda > 500$ nm). There is an initial induction period where oxygen formation is not observed, followed by a period of steady O_2 evolution. Eventually, the rate of O_2 evolution decreases, primarily owing to the deposition of metallic silver on the photocatalyst as the result of Ag^+ reduction (Figure S8). This is commonly observed in water oxidation reactions that use Ag^+ as an electron acceptor.[15–18,29–32] When the reaction was conducted with 50 mg of 3.0 wt% $Co(OH)_2/TiO_2$ in a similar manner, approximately 27 μmol of O_2 had been produced after 15 h of irradiation (Figure S9). In this case, the amount of O_2 produced was 1.7 times greater than the $Co(OH)_2$ loading. These results confirm that the reaction is not stoichiometric, but catalytic.

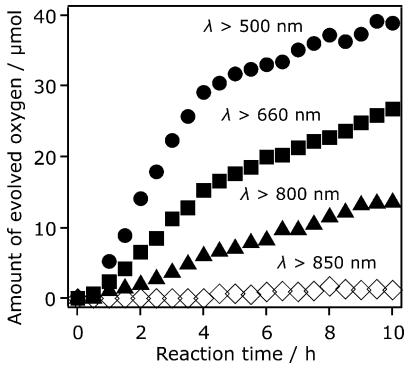

Figure 5. Time dependence of the O_2 evolution for 3.0 wt% $Co(OH)_2/TiO_2$ under visible-light irradiation at different wavelengths. Reaction conditions: Catalyst (100 mg), reactant solution, aqueous silver nitrate solution (10 mM, 140 mL) containing 200 mg of La_2O_3, 300 W xenon lamp with a cut off filter.

Figure 5 also shows that the O_2 evolution activity of 3.0 wt% $Co(OH)_2/TiO_2$ decreased as the wavelength of the incident light was increased. Under >850 nm irradiation, the O_2 evolution rate became negligible. The longest wavelength at which the photocatalytic reaction occurred was 850 nm, which corresponds to the absorption edge for $Co(OH)_2/TiO_2$. This result clearly indicates that the reaction is activated by the absorption of the incident light. The AQE was calculated to be approximately 0.09% at 500 nm irradiation under the optimized conditions (Figure S10).

For comparison, photocatalytic water oxidation was also conducted with the benchmark photocatalysts WO_3 and TaON, which work under visible-light irradiation with AQEs of about 10–30%.[35,36] Under irradiation at wavelengths of greater than 440 nm, where these reference materials are all photoexcited, O_2 evolution was observed. However, their activity became almost zero at wavelengths greater than 660 nm because these reference materials do not absorb $\lambda > 660$ nm light owing to their large band gaps (Figures S11 and S12). Thus it was shown that the $Co(OH)_2/TiO_2$ photocatalyst outperforms existing benchmark photocatalysts with respect to the absorption in the visible range. Nevertheless, both WO_3 and TaON became active under >660 nm irradiation when modified with $Co(OH)_2$ owing to the new absorption bands generated by $Co(OH)_2$ although they were not as active as $Co(OH)_2/TiO_2$.

Our strategy to use $Co(OH)_2$ towards visible-light water oxidation could be applicable to some other wide-band-gap oxide semiconductors (Table S2 and Figure S13). Although these systems have not yet been optimized, our results suggest the general applicability of this strategy not only to metal oxides but also to oxynitrides for harvesting longer-wavelength photons. However, we note that there were some unsuccessful examples; for example, O_2 evolution was negligible using $Co(OH)_2/ZnO$, which is presumably due to the inherent instability of ZnO in an aqueous environment. We also tested $Co(OH)_2/SnO_2$, which showed O_2 formation upon visible-light irradiation (>500 nm), but the activity was much lower compared to those achieved with other materials (Table S2 and Figure S13). A possible explanation for the low activity is that O_2 reduction, the undesired backward reaction, might occur efficiently on SnO_2. Oxygen vacancies are known to act as active sites for O_2 reduction,[37] and SnO_2 has a relatively high concentration of oxygen vacancies. Therefore, we surmised that O_2 reduction also occurred on SnO_2 during the water oxidation reaction, which contributed to the lower O_2 evolution.

In summary, we have shown that rutile TiO_2 nanorods decorated with $Co(OH)_2$ nanoclusters, prepared by a simple soft chemical process, are suitable catalysts for water oxidation under visible-light irradiation at wavelengths of up to 850 nm. Most reported metal oxide photocatalysts are inactive at such wavelengths ($\lambda > 400$ nm), which is primarily due to their large band gaps of greater than 3.0 eV. To the best of our knowledge, this is the first example of a particulate photocatalyst that is capable of catalyzing water oxidation at such long wavelengths. The $Co(OH)_2$ nanoclusters were found to serve as both water oxidation catalysts and visible-light absorption centers. This raises the possibility that such cobalt-based nanoclusters may also serve to activate other wide-band-gap metal oxides, enabling them to harvest visible

 © 2016 Wiley-VCH Verlag GmbH & Co. KGaA, Weinheim

light and oxidize water. This will be a subject for future research.

Acknowledgements

This work was supported by Grants-in-Aid for Challenging Exploratory Research (15K14220), Young Scientists (A) (25709078), and by the Scientific Research on Innovative Areas program (25107512; AnApple). We would also like to acknowledge the Hosokawa Powder Technology Foundation, The Noguchi Institute, and the PRESTO/JST program "Chemical Conversion of Light Energy".

Keywords: heterogeneous catalysis · photocatalysis · semiconductors · solar energy · water oxidation

How to cite: *Angew. Chem. Int. Ed.* **2016**, *55*, 8309–8313
Angew. Chem. **2016**, *128*, 8449–8453

[1] A. Fujishima, K. Honda, *Nature* **1972**, *238*, 37–38.
[2] K. Maeda, K. Teramura, D. Lu, T. Takata, N. Saito, Y. Inoue, K. Domen, *Nature* **2006**, *440*, 295.
[3] X. Wang, K. Maeda, A. Thomas, K. Takanabe, G. Xin, J. Carlsson, M. K. Domen, M. Antonietti, *Nat. Mater.* **2009**, *8*, 76–80.
[4] X. Xu, C. Randorn, P. Efstathiou, J. T. S. Irvine, *Nat. Mater.* **2012**, *11*, 595–598.
[5] Y. Umena, K. Kawakami, J.-R. Shen, N. Kamiya, *Nature* **2011**, *473*, 55–60.
[6] V. Artero, M. Chavarot-Kerlidou, M. Fontecave, *Angew. Chem. Int. Ed.* **2011**, *50*, 7238–7266; *Angew. Chem.* **2011**, *123*, 7376–7405.
[7] L. Duan, F. Bozoglian, S. Mandal, B. Stewart, T. Privalov, A. Llobet, L. Sun, *Nat. Chem.* **2012**, *4*, 418–423.
[8] M. W. Kanan, Y. Surendranath, D. G. Nocera, *Chem. Soc. Rev.* **2009**, *38*, 109–114.
[9] M. Zhang, M. de Respinis, H. Frei, *Nat. Chem.* **2014**, *6*, 362–367.
[10] a) A. Kudo, Y. Miseki, *Chem. Soc. Rev.* **2009**, *38*, 253–278; b) K. Maeda, K. Domen, *J. Phys. Chem. Lett.* **2010**, *1*, 2656–2661.
[11] a) J. Sato, N. Saito, N. Nishiyama, Y. Inoue, *J. Phys. Chem. B* **2003**, *107*, 7965–7969; b) H. Kato, K. Asakura, A. Kudo, *J. Am. Chem. Soc.* **2003**, *125*, 3082–3089; c) K. Maeda, *Chem. Commun.* **2013**, *49*, 8404–8406; d) Y. Sakata, T. Hayashi, R. Yasunaga, N. Yanaga, H. Imamura, *Chem. Commun.* **2015**, *51*, 12935–12938.
[12] D. E. Scaife, *Sol. Energy* **1980**, *25*, 41–54.
[13] Y. Miseki, H. Kusama, H. Sugihara, K. Sayama, *Chem. Lett.* **2010**, *39*, 846–847.
[14] K. Maeda, K. Domen, *J. Phys. Chem. C* **2007**, *111*, 7851–7861.
[15] a) F. Zhang, A. Yamakata, K. Maeda, Y. Moriya, T. Takata, J. Kubota, K. Teshima, S. Oishi, K. Domen, *J. Am. Chem. Soc.* **2012**, *134*, 8348–8351; b) S. Chen, S. Shen, G. Liu, Y. Qi, F. Zhang, C. Li, *Angew. Chem. Int. Ed.* **2015**, *54*, 3047–3051; *Angew. Chem.* **2015**, *127*, 3090–3094.
[16] K. Maeda, M. Higashi, B. Siritanaratkul, R. Abe, K. Domen, *J. Am. Chem. Soc.* **2011**, *133*, 12334–12337.
[17] a) K. Maeda, K. Domen, *Angew. Chem. Int. Ed.* **2012**, *51*, 9865–9869; *Angew. Chem.* **2012**, *124*, 10003–10007; b) K. Maeda, D. Lu, K. Domen, *Angew. Chem. Int. Ed.* **2013**, *52*, 6488–6491; *Angew. Chem.* **2013**, *125*, 6616–6619.
[18] T. Hisatomi, C. Katayama, Y. Moriya, T. Minegishi, M. Katayama, H. Nishiyama, T. Yamada, K. Domen, *Energy Environ. Sci.* **2013**, *6*, 3595–3599.
[19] M. W. Kanan, D. G. Nocera, *Science* **2008**, *321*, 1072–1075.
[20] F. Jiao, H. Frei, *Angew. Chem. Int. Ed.* **2009**, *48*, 1841–1844; *Angew. Chem.* **2009**, *121*, 1873–1876.
[21] G. Zhang, S. Zang, X. Wang, *ACS Catal.* **2015**, *5*, 941–947.
[22] T. Zidki, L. Zhang, V. Shafirovich, S. V. Lymar, *J. Am. Chem. Soc.* **2012**, *134*, 14275–14278.
[23] J. B. Gerken, J. G. McAlpin, J. Y. C. Chen, M. L. Rigsby, W. H. Casey, R. D. Britt, S. S. Stahl, *J. Am. Chem. Soc.* **2011**, *133*, 14431–14442.
[24] M. Barroso, A. J. Cowan, S. R. Pendlebury, M. Grätzel, D. R. Klug, J. R. Durrant, *J. Am. Chem. Soc.* **2011**, *133*, 14868–14871.
[25] M. Higashi, K. Domen, R. Abe, *J. Am. Chem. Soc.* **2012**, *134*, 6968–6971.
[26] J. R. S. Brownson, C. Lévy-Clément, *Electrochim. Acta* **2009**, *54*, 6637–6644.
[27] J. Yang, T. Sasaki, *Chem. Mater.* **2008**, *20*, 2049–2056.
[28] The spectral shape of Co $2p_{3/2}$ in the prepared samples is similar to that of a bulk $Co(OH)_2$ reference compound, which further supports our claim that the loaded Co species on TiO_2 is mainly $Co(OH)_2$.
[29] A. Kudo, K. Omori, H. Kato, *J. Am. Chem. Soc.* **1999**, *121*, 11459–11467.
[30] A. Ishikawa, T. Takata, J. N. Kondo, M. Hara, H. Kobayashi, K. Domen, *J. Am. Chem. Soc.* **2002**, *124*, 13547–13553.
[31] a) H. G. Kim, D. W. Hwang, J. S. Lee, *J. Am. Chem. Soc.* **2004**, *126*, 8912–8913; b) H. G. Kim, P. H. Borse, W. Choi, J. S. Lee, *Angew. Chem. Int. Ed.* **2005**, *44*, 4585–4589; *Angew. Chem.* **2005**, *117*, 4661–4665.
[32] Z. Yi, J. H. Ye, N. Kikugawa, T. Kako, S. Ouyang, H. Stuart-Williams, H. Yang, J. Y. Cao, W. J. Luo, Z. S. Li, Y. Liu, R. L. Withers, *Nat. Mater.* **2010**, *9*, 559–564.
[33] K. Maeda, *Chem. Lett.* **2015**, *44*, 934–936.
[34] L. Kavan, M. Grätzel, S. E. Gilbert, C. Klemenz, H. J. Scheel, *J. Am. Chem. Soc.* **1996**, *118*, 6716–6723.
[35] G. Hitoki, T. Takata, J. N. Kondo, M. Hara, H. Kobayashi, K. Domen, *Chem. Commun.* **2002**, 1698–1699.
[36] S. S. K. Ma, K. Maeda, R. Abe, K. Domen, *Energy Environ. Sci.* **2012**, *5*, 8390–8397.
[37] a) J. Seo, D. Cha, K. Takanabe, J. Kubota, K. Domen, *ACS Catal.* **2013**, *3*, 2181–2189; b) T. Arashi, J. Seo, K. Takanabe, J. Kubota, K. Domen, *Catal. Today* **2014**, *233*, 181–186; c) A. Ishihara, M. Tamura, Y. Ohgi, M. Matsumoto, K. Matsuzawa, S, Mitsushima, H. Imai, K. Ota, *J. Phys. Chem. C* **2013**, *117*, 18837–18844.

Received: March 18, 2016
Revised: May 1, 2016
Published online: May 25, 2016

 © 2016 Wiley-VCH Verlag GmbH & Co. KGaA, Weinheim